Environ. Sci. Technol. **2004**, *38,* 5253−5260

Chemical Structure of Arsenic and Chromium in CCA-Treated Wood: Implications of Environmental Weathering

PETER S. NICO,*,† SCOTT E. FENDORF,‡ YVETTE W. LOWNEY,§ STEWART E. HOLM,# AND MICHAEL V. RUBY§

Chemistry Department, California State University, Stanislaus, 801 West Monte Vista Boulevard, Turlock, California 95382, Geological and Environmental Sciences, Stanford University, Stanford, California 94305, Exponent, Boulder, Colorado 80301, and Georgia-Pacific Corporation, Atlanta, Georgia 30035

Chromated copper arsenate (CCA) has been used to treat lumber for over 60 years to increase the expected lifetime of CCA-treated wood. Because of the toxicity of the arsenic and chromium used in CCA treatment, regulatory and public attention has become focused on the potential risks from this exposure source. In particular, exposure of children to arsenic from CCA-treated wood used in decks and play sets has received considerable attention. X-ray Absorption Spectroscopy (XAS) was used to evaluate the chemical structure of As and Cr in three samples of CCA-treated materials: newly treated wood, aged wood (5 years as decking), and dislodgeable residue from aged (1−4 years as decking) CCA-treated wood. The form of the Cr and As in CCA-treated material is the same in fresh and aged samples, and between treated wood and dislodged residue. In all cases, the dominant oxidation state of the two elements is As(V) and Cr(III), and the local chemical environment of the two elements is best represented as a Cr/As cluster consisting of a Cr dimer bridged by an As(V) oxyanion. Long-term stability of the As/Cr cluster is suggested by its persistence from the new wood through the aged wood and the dislodgeable residue.

Introduction

Chromated copper arsenate (CCA) has been used to treat lumber for over 60 years (*1*), owing to the extended lifetime of CCA-treated wood as compared to its untreated counterparts (*2*−*5*). Since the late 1980s, U.S. production of CCA-treated lumber has averaged approximately 5×10^8 ft^3/yr (*6*). Because of the inherent toxicity of the arsenic and chromium used in CCA treatment, regulatory and public attention has become focused on the potential risks from this exposure source. In particular, exposure of children to arsenic from CCA-treated wood used in decks and play sets has received considerable attention. As a result, the U.S. EPA Office of Pesticide Programs (OPP) is currently preparing a human health risk assessment for direct-contact exposures to CCA-treated wood (www.epa.gov).

The chemical and structural environment of arsenic and chromium in CCA-treated wood has been speculated (*2*, *3*, *7*−*9*) but remains unresolved. Bull et al. (*2*) performed the most extensive investigation to date, concluding that As and Cr are present in the (V) and (III) oxidation states, respectively, and that all of the As and half of the Cr were present in the solid $CrAsO_4$. They further reasoned that the remaining Cr must be present as $Cr(OH)_3$(s). X-ray diffraction analysis of CCA-treated material showed no detectable crystalline phases other than that of the wood cellulose (*8*, *9*).

Previous studies (as mentioned above) were conducted using newly prepared CCA-treated wood. To the best of our knowledge, there has been no comprehensive study of the changes in Cr and As that occur over time as these materials are exposed to the environment. Accordingly, this research addresses the chemical nature and form (structure) of arsenic and chromium in CCA-treated wood, and whether the chemical environment changes with time and weathering. Understanding the chemical and structural state of Cr and As within the treated wood will suggest the likely magnitude of human exposures to As and Cr from CCA-treated wood and the possible fate and transport of these elements in the environment. In regards to exposure, a primary question is whether arsenic from CCA-treated wood is absorbed to the same extent as soluble arsenic, or whether the binding of arsenic in the CCA chemical complex results in lower oral and dermal absorption (relative to soluble arsenic). To this end, a companion study is underway, using the same substrates described in this study, to assess the oral and dermal absorption of arsenic from the CCA-treated wood. However, to design appropriate exposure studies, it is necessary to understand the chemical state of arsenic in CCA-treated wood, and whether environmental weathering can result in a change over time to this chemical state.

Here, we evaluated the As and Cr chemistry in three CCA-treated wood samples: newly treated wood, aged wood, and dislodgeable residue from aged CCA-treated wood. The chemistry of Cu in CCA materials was not explored in this work because Cu has a generally lower toxicity than As or Cr and has therefore not received the same regulatory attention.

The dislodgeable residue was used to assess the oral and dermal absorption of arsenic from CCA-treated wood. X-ray Absorption Spectroscopy (XAS) was used to determine the chemical and structural environment of the Cr and As in these materials. XAS is ideally suited for this type of analysis because it requires no chemical manipulation of the samples and is not limited to crystalline structures. Manipulation of the sample, such as chemical extraction, increases the potential for unintentional alteration of the Cr and As oxidation state or chemical environment during analysis.

Materials and Methods

XAS was used to analyze samples from (*1*) newly treated wood, (*2*) wood collected from a deck that had been subjected to natural environmental weathering for 5 years (aged wood), and (*3*) residue collected from CCA-treated wood. Additionally, an X-ray microprobe was used to examine new and aged wood to determine element distributions. Finally, total elemental concentrations of As, Cr, Cu, Fe, and Mn were determined on digests of the solids using inductively coupled plasma/mass spectroscopy (ICP/MS). The wood samples were digested in refluxing nitric acid until no visible solid

* Corresponding author phone (209)667-3384; fax: (209)667-3845; e-mail: nico@chem.csustan.edu.
† California State University.
‡ Stanford University.
§ Exponent,
# Georgia-Pacific Corporation.

10.1021/es0351342 CCC: $27.50
Published on Web 09/03/2004

material remained and a clear, straw-colored extract was obtained. The digests were then analyzed for metal concentrations by ICP/MS. This work was performed at Columbia Analytical Services in Kelso, Washington. Duplicate wood samples were digested, resulting in relative percent differences (RPDs) ranging from 1.2% to 2.5% for arsenic, chromium, and copper. In addition, a sample of the wood material was sent to an independent laboratory (Battelle Columbus) where it was analyzed for arsenic, chromium, and copper concentrations by the same method. The independent analysis was within 10% of the concentrations of arsenic, chromium, and copper in the wood sample, as reported by Columbia Analytical.

For the two solid wood samples (fresh and aged), a 2- × 3- × 1-cm subsection of the wood was removed for analysis (the top side of the weathered CCA-treated wood was used). The aged wood was Southern Yellow Pine that came from decks in Pennsylvania or in Atlanta, Georgia, and had been in service for at least 4 years. The residue used in this study, in the form of a fine particulate, was supplied by the American Chemistry Council's CCA-Treated Wood Group. The sample was derived from CCA-treated boards that were removed from in-service residential decks in Michigan and Georgia where they were subject to ambient weathering conditions, and consisted of either Southern Yellow Pine or Ponderosa Pine. Deck structures had been weathered in the environment for 1 to 4 years and had no coatings applied. A total of 1,456 board sections (each 2 ft long) were collected and shipped to Michigan State University, where the dislodgeable material was collected as a single composite from multiple boards. The dislodgeable material was collected by brushing the board with a soft-bristle test tube brush while rinsing with DI water. The effluent and particulate were filtered through glass wool, concentrated by rotary evaporation under vacuum at 46 °C, and then air-dried in a fume hood at 22 °C. The dislodgeable residue was a fine powder and was therefore packed into a Plexiglass sample holder and covered with Kapton tape.

Bulk-phase Cr and As K-edge spectra of both the near-edge (XANES) and extended fine-structure (EXAFS) were collected on beamline 4−3, an 8-pole wiggler, with an approximate 20 × 4 mm beam size, at the Stanford Synchrotron Radiation Laboratory. The ring operated at ∼3 GeV, with a current ranging from ∼100 to 50 mA. Spectra were collected in fluorescence mode using a 13-element solid-state detector and a Si (220) monochromator. Incident and transmitted intensities were measured with in-line ionization chambers. Energy calibration was achieved by analyzing a Cr metallic foil before collecting the sample in the case of Cr, and by simultaneously recording the transmission spectra for an internal As(V) standard, Na_3AsO_4, in the case of As.

Fluorescence spectra were processed using SixPack, a comprehensive XAS data reduction and modeling program (designed and provided by Dr. S. Webb, SSRL) (*10*). Basic signal processing included averaging of individual scans, background subtraction, normalization of the edge jump to unity, and extraction of the EXAFS oscillations though the subtraction of a spline function. Spectra were then converted from eV to k (A^{-1}) units to produce an EXAFS ([χ(k)]) function.

Conventional EXAFS fitting was performed using the WinXAS 2.1 data analysis routine (*11*). Chi functions were k^3 weighted and Fourier transformed to real (R) space. Individual scattering paths were generated using Feff 7 (*32*), a curved-wave, multiscatter ab initio code for X-ray absorption phenomena. Fits were initially optimized in R space, but the final refinement was always performed on the original EXAFS data. Fitting of the As and Cr EXAFS spectra was broken into stages. The oxygen shells were fitted first with second-shell backscatters and multiple scattering paths being added later. Actually fit minimizations were preformed in an iterative manor. Initial guesses were entered for coordination numbers (N), bond distances, and Debye−Waller factors (σ^2). The E_0 shifts were equated for all shells and allowed to float. After this the E_0's were locked and the coordination numbers, bond distances, or Debye−Waller factors were allowed to float. (Coordination numbers and distances for multiple scatter paths were always maintained at theoretically defined values) Coordination numbers and Debye−Waller factors were never allowed to vary simultaneously to avoid artifacts induced by correlation of these two parameters. This process was reiterated until all values became stable. The process was then repeated from a different initial guess to make sure the same values were converged upon. The C shell in the Cr EXAFS was added only after all the other backscatters had been added to the model and stable sets of parameters had been converged upon. All other parameters were held constant while the C parameters were fitted in the same iterative manor described above. Once the C parameters were stable, parameters for the other shells were allowed to float in various combinations to make sure that the presence of the new carbon shell did not alter the previously stable parameters. Although the contribution from the C shell is small, due to the fact that C is a small backscatter, the C contribution was included in the model because it improved the overall quality of the fits, stabilized at reasonable values similar to those seen in other comparable EXAFS studies, and because of the chemical arguments that can be made for its presence in the Cr coordination shells. These chemical arguments and previous work are outlined in detail below.

X-ray microprobe mapping was done on beamline 10.3.2 at the Advanced Light Source, Lawrence Berkeley National Laboratory. Samples were run in fluorescence mode using a six-element solid state Ge detector. The beam size was approximately 17 × 5 microns, and the X-ray energy was 13 000 eV.

Energy minimization of the proposed cluster was done using Spartan ′02. (Copyright 1991−2002 by WaveFunction Inc.) The minimization was done at the molecular mechanics level of theory.

Results and Discussion

No significant differences were present between the XANES and EXAFS spectra for the three samples (freshly treated wood, aged wood, and dislodgeable residue), Figure 1. Because of the similarity in the spectra and the expected greater importance of the dislodgeable residue in human exposures, the latter material was used to determine the chemical and structural state of arsenic and chromium.

Metal Concentrations. The average concentration of arsenic in the residue was 47.5 mmol/kg, while that of chromium was 78.8 mmol/kg (Table 1). This equates to a Cr:As molar ratio of 1.7:1. In the freshly treated wood, the Cr:As molar ratio was 1.5:1, while in the aged treated wood it increased to 2.2:1. The residue also contains approximately 100-fold more iron than either the newly treated or the aged treated wood. This appears to result from soil minerals (including iron phases) that accumulated on the decks, and was then liberated during the collection of the dislodgeable residue.

Oxidation State/Chemical Environment. The absorption edge for arsenic was ca. 11 874 eV, which is indicative of the As(V) oxidation state (as noted by its comparison to the arsenate standard; Figure 1a). Similar comparisons showed that the As in the new and aged wood samples is also As(V). The absence of a distinct preedge feature, which would result for chromate, indicates that the Cr is present solely in the Cr(III) oxidation state, as is the case for the new and aged wood samples (Figure 1b). Figures 2a and 3a show the As and Cr EXAFS functions, respectively, of the three different

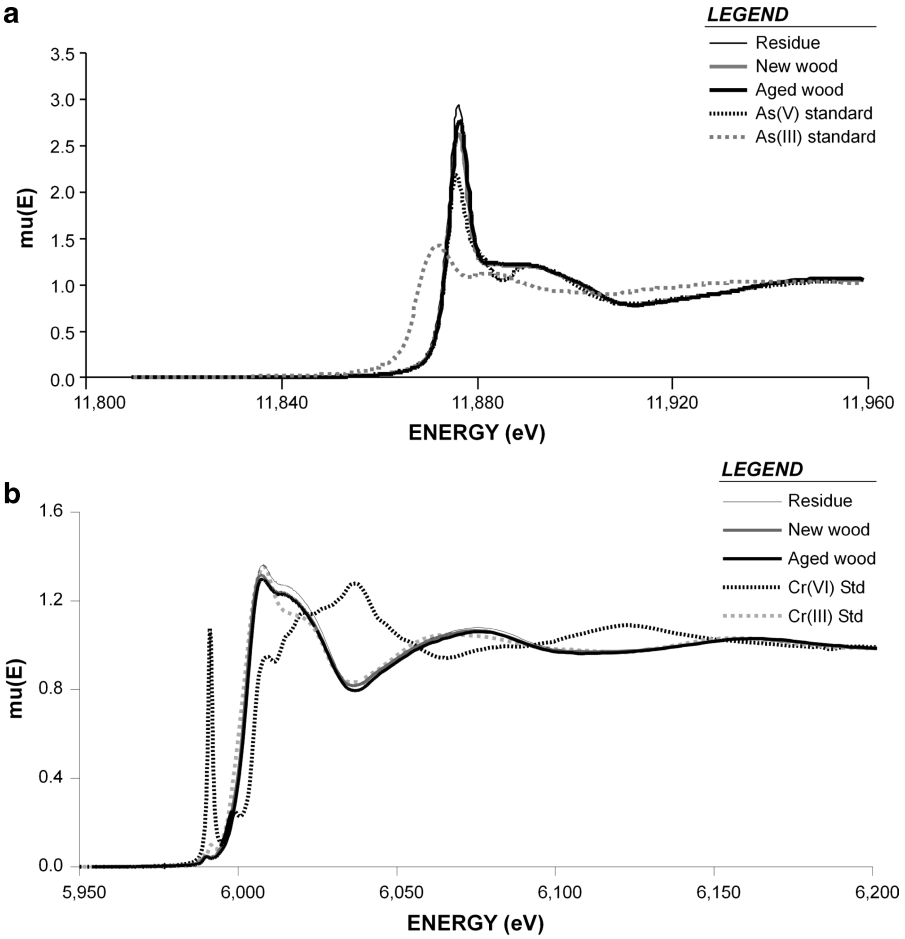

FIGURE 1. (a) As XANES spectra of the three samples, including an As(III) and an As(V) standard. (b) Cr XANES spectra of the three samples, including a Cr(III) and a Cr(VI) standard.

TABLE 1. Total Metals Concentrations in CCA Treated Materials

	As (mmol/kg)	Cr (mmol/kg)	Cu (mmol/kg)	Fe (mmol/kg)	Mn (mmol/kg)
fresh wood	31.5	48.6	22.8	0.57	0.26
aged wood	23.5	51.9	14.8	3.12	0.2
residue	47.5	78.8	35.3	268	3.49

wood samples. No significant difference is observable between the three samples.

Chemical Environment. The two most prominent features in the Fourier transform of the As EXAFS are the two peaks at 1.27 Å and 2.8 Å (distances are uncorrected for phase shifts) (Figure 2c). The first peak was best fitted by a shell of 3.9 oxygen atoms at a distance of 1.68 Å (Figure 2c; Table 2). This is in excellent agreement with the expected values for a tetrahedrally oxygen-coordinated As(V) species, as AsO_4^{3-} (*12*, *13*), and confirms As(V) as the dominant As oxidation state. The peak at 2.8 Å was fitted with a shell of 1.9 chromium atoms at a distance of 3.25 Å (Figure 2c; Table 2). Two multiple scattering paths, namely As−O−O and As−O−As−O, were also included in the fitting procedure. The coordination number and distances for the multiple scattering paths were constrained to atomic positions, which varied with the single scattering paths. Consequently, the only additional degrees of freedom introduced by the inclusion of these two paths were their respective σ^2 constants.

In the Cr Fourier transform spectrum of the easily dislodgeable residue, there are again two distinct features, denoted as the low-distant and high-distant peaks in Figure 3a. The low-distant peak (centered at 1.6 Å but uncorrected for phase shift) is fitted well by a shell of 6.0 oxygen atoms at a distance of 1.97 Å (Figure 3a). These values compare well with those expected for octahedral oxygen-coordinated Cr(III). Again, analysis of the EXAFS spectra supports the XANES data, indicating Cr(III) as the sole oxidation state of this element. The higher-distant peak(s) are a mixture of three distinct shells that are described by 1.3 As at 3.25 Å, 1.2 Cr at 3.47 Å, and 4.7 C at 3.08 Å (Table 2; Figure 3a). The Cr EXAFS analysis thus provides additional evidence for the d(Cr−As) of 3.25 Å, corroborating that of the As spectra. Addition of a Cr−O−Cr−O multiple-scattering shell qualitatively improved the fits, but the improvement was not statistically significant given the increased degrees of freedom. Consequently, these paths were omitted from the final fitting procedure. A similar situation was encountered by allowing the Cr−O distances in the first oxygen shell to take on two independent scattering distances.

Since there is a large amount of iron present in the residue, and because Cr and Fe are similar in size and backscattering properties, they cannot be distinguished by EXAFS spectroscopy. Thus, the possibility that the Cr backscatter signals seen in both the As and Cr EXAFS are partially due to Fe must be considered. These are complex and heterogeneous systems, especially the residue, and it is to be expected that there are many minor species present. Minor species are responsible for, among other things, the lack of perfect agreement between the experimental EXAFS spectra and the theoretical fits shown in Figures 2b and 3b. Therefore, it is possible (and maybe even probable) that some fraction of the Cr in the residue is bound to Fe, and similarly, that some of the As is bound to either pure Fe phases and/or to mixed

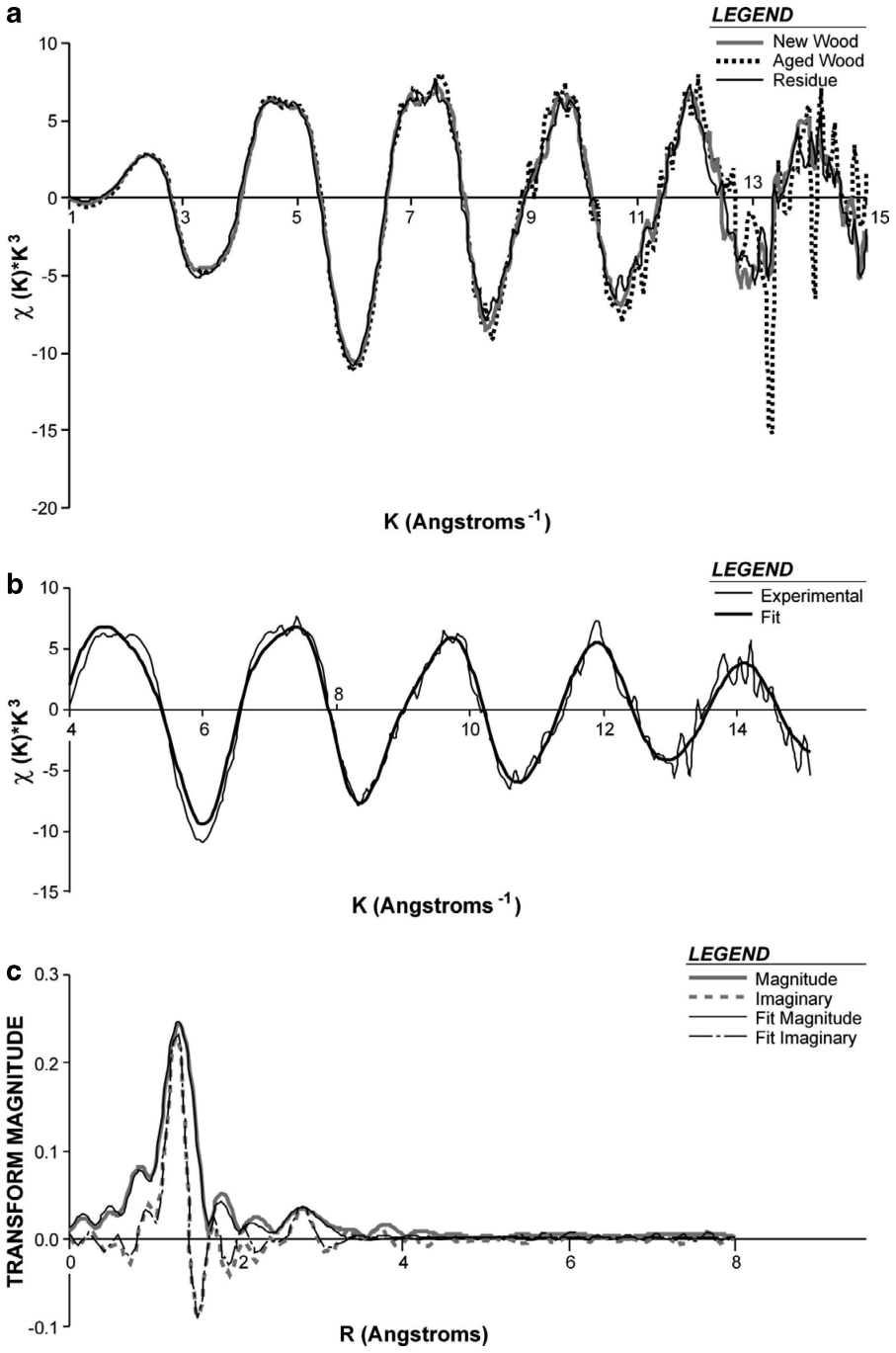

FIGURE 2. (a) Comparison of As EXAFS functions from three different samples (aged, unaged, residue) showing no significant differences. (b) As EXAFS function and (c) Fourier transform from residue sample, showing experimental data and fits.

TABLE 2. Final Cr and As EXAFS Fitting Parameters

	As EXAFS ($S_0^2 = 0.99$)				Cr EXAFS ($S_0^2 = 0.64$)			
scattering pair	As−O	As−Cr	As−O −O	As−O−As−O	Cr−O	Cr−C	Cr−As	Cr−Cr
coordination number (N)	3.9	1.9	12	4	6.0	4.74	1.27	1.18
distance R (Å)	1.68	3.25	3.06	3.36	1.97	3.08	3.25	3.47
σ^2	0.0022	0.0094	0.005 3	0.01	0.0016	0.011	0.0018	0.0017
E_0	0.82	0.82	0.82	0.82	−2.41	−2.41	−2.41	−2.41

Cr/Fe phases. However, we conclude that the Cr shells were the best-fitting choices and the dominant backscattering species for the following reasons. One, the substitution of Fe for Cr in the fitting procedure caused the fits to be slightly worse. Two, the similarity between the EXAFS spectra of the residue and of the new and aged wood, in which there is very little Fe, strongly implies that the major species in all three systems is the same. The lack of iron, manganese, or other similar Z elements in these two wood samples requires that Cr be the dominant backscatterer in these systems. Therefore, Cr is most likely to be the dominant backscatterer in the residue as well.

The presence of a Cr backscatterer in the Cr EXAFS is in good agreement with Cr(III)'s well-known tendency to

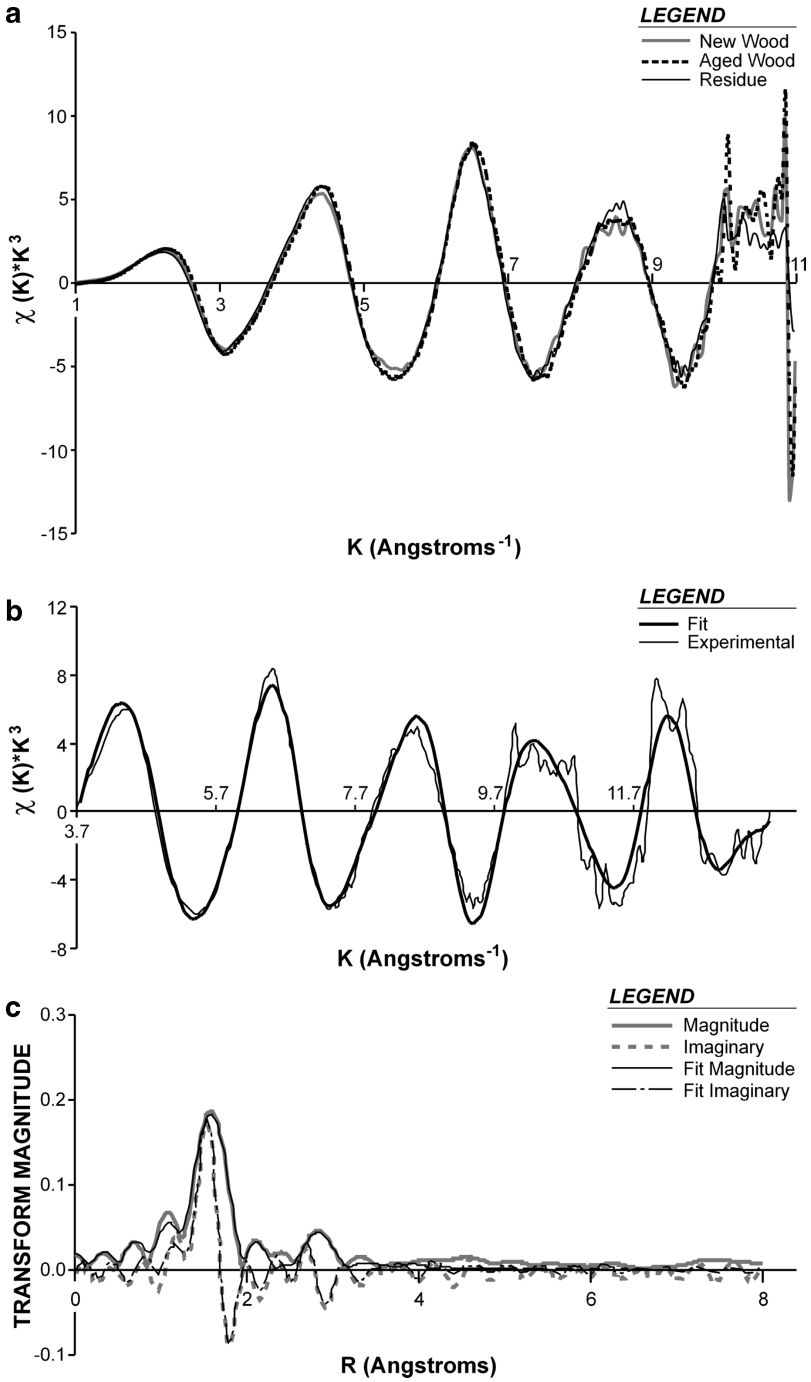

FIGURE 3. (a) Comparison of Cr EXAFS functions from three different samples (aged, unaged, residue), showing no significant differences. (b) Cr EXAFS function and (c) Fourier transform from residue sample, showing experimental data and fits.

polymerize into dimers or large n-polymers (*14*−*24*). The Cr−Cr distance is relatively long, 3.47 Å, indicating that the two Cr atoms are probably bridged by one or more ligands other than oxygen. In the investigation of over 26 Cr dimers, Stearns and Armstrong (*15*) found that, in all cases, dimers that were bridged by two μ-O's had Cr−Cr distances in the 2.95 to 3.09 Å range. Similarly, Cr−Cr distances for Cr pairs bridged by a μ-O and two carboxyl groups range from 3.38 to 3.42 Å (*17, 18*). Our observed Cr−Cr distance is slightly longer than this range, implying that the Cr dimer is bridged by at least two non μ-O groups. The obvious possibilities for these groups would be either the As tetrahedral and/or oxygen-containing ligands present in the wood structure. Several studies of Cr binding to other biological organic ligands, such as oat biomass (*25*), hops biomass (*26*), brown seaweed biomass (*27*), and straw lignin (*28*), show that Cr binds strongly to these organic substrates and that carboxyl groups on the substrate are the most likely binding sites. Additionally, the presence of carbon as a minor backscatterer in the Cr EXAFS strongly implies that the Cr−As complex is bound directly through innersphere complexes to the wood structure (through the Cr component). The EXAFS-derived Cr−C coordination number (4.7) and distance (3.08 Å) are similar to those found in an EXAFS investigation of Cr binding by Chromodulin, an oligopeptide known for its strong Cr binding properties (*20*). For Chromodulin, C coordination numbers ranged from 4 to 5.5 carbon atoms and distances ranged from 2.98 to 3.12 Å (*20*). Similarly, the crystallographically derived Cr−C distance for Cr pairs bridged by two acetate ligands ranges from 2.93 to 3.04 Å (*17, 18*).

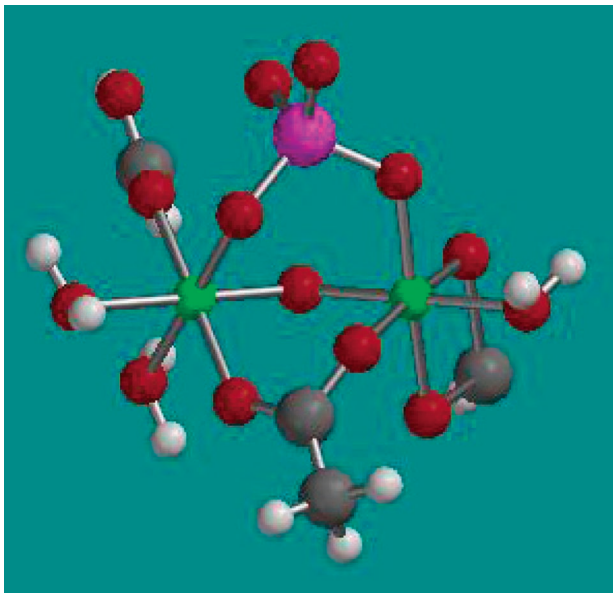

FIGURE 4. Model of Cr/As cluster with distances constrained to distances from EXAFS fits and then minimized using molecular mechanics minimization. Oxygen atoms are shown in red, Cr atoms in green, carbon in gray, hydrogen in white, and As in large orange.

The As−Cr distance of 3.25 Å seen in both the Cr and As EXAFS spectra is very similar to that for a binuclear, bidentate As−Fe complex (i.e., an As tetrahedral bridging an Fe pair, a double corner sharing) (*13*). Given the similar size and chemical properties of Cr and Fe, we conclude that the As in this system is most likely bound to Cr in a similar manor, and we therefore propose a model for the dominant form of the Cr and As in these CCA-treated materials (Figure 4)-the model was constructed using the bonding environment derived from the XAS data that had been refined using molecular mechanics to minimize the structural energy. Because of the necessity for computational simplicity, the carboxyl groups of the wood structure were modeled by either a simple acetate group in the case of the bridging ligand or by formic acid groups in the case of the two example Cr chelating ligands. The molecular mechanical energy minimization shows that the proposed structure is chemically feasible but results in the twisting of the As and acetate bridges to reduced steric interactions. While the bridging acetate ligand is thought to be an integral part of the structure, the two other oxygen-containing organic ligands are included simply as examples of possible ligation schemes and are not intended to represent any specific binding mode. Furthermore, even though carboxylate ligands are excellent Cr-chelating ligands, there are also many other oxygen-containing functional groups present in the wood structure that could bind the Cr. The waters of hydration shown in Figure 4 are also not intended to be an essential element of the proposed model; while it is perfectly possible that the Cr retains some waters of hydration, it is also possible that these could be replaced by hydroxide ions or other oxygen-containing ligands present in the system. The Cr−O distances in the minimized structure are all between 1.9 and 2.1 Å. A similar level of oxygen disorder is seen in the crystal structures of many different Cr clusters (*17*−*19*, *21*, *23*).

The proposed Cr/As cluster model is in good agreement with the Cr-to-As molar ratio present in the residue and the aged wood sample, 1.7:1 and 2.2:1, respectively. Similarly, it is in excellent agreement with the 2:1 Cr-to-As molar ratio present in the initial CCA treating solution (*2*). This model also conforms to the observed lack of crystallinity in CCA-treated material (*8*, *9*). Furthermore, it is in partial agreement with the $CrAsO_4$ model put forth by Bull et al. (*2*), to the extent that it shows the As bound to Cr; the structure of the complex is likely very similar between these two studies. Our proposed structure, however accounts for the Cr:As ratio, whereas Bull et al. (*2*) postulated an additional fraction of $Cr(OH)_3$. Similarly, As coprecipitated with or adsorbed on ferric hydroxide shows a comparable binuclear bidentate structures (*13*). The Cr/As cluster size within the CCA-treated wood remains unresolved, and it is possible that differing numbers of clusters could be linked to create a range of sizes.

Distributions of Cr, Cu, and As in the aged wood samples, obtained using an X-ray microprobe, show a relatively uniform distribution (Figure 5). The greatest differences in intensity are well correlated with the changes in density observed in the wood grain (Figure 5d). The uniform distribution of Cr and As throughout the sample further supports the Cr/As cluster model proposed above. If the samples contained localized elemental deposition (as small as ca. 0.5 μm in diameter), these would be observed. The

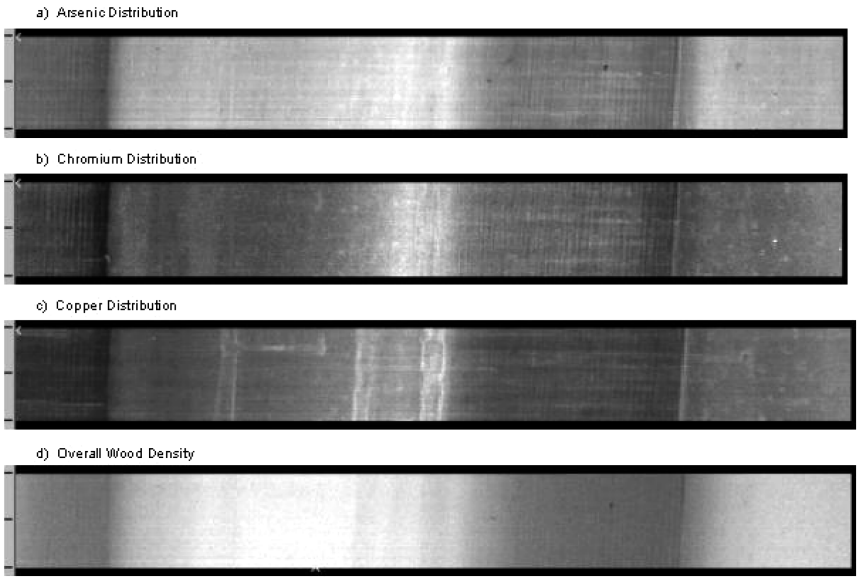

FIGURE 5. (a−d) A 10 × 1 mm micro-XAS map showing (a) As distribution, (b) Cr distribution, (c) Cu distribution, (d) backscatter peak, which serves as general density (can see wood grain). Brighter areas are those with higher concentrations of metal (A, B, C) or greater density of wood (D).

correlation between the fluorescence intensity of the Cr and As (Figure available in Supporting Information) shows two distinct data clusters, with one cluster corresponding exclusively to the low-density areas of the wood and the other to the high-density areas. Both clusters show a strong As to Cr linear relationship, $r = 0.982$ and 0.963, respectively, with identical slopes, $m = 0.05$, implying a uniform Cr-to-As ratio throughout the wood sample.

Although the exact reaction mechanism between the CCA-treated solution and the wood structure is undoubtedly complex and varied, a general reaction scheme can be proposed that conforms to the results discussed above. The first steps in the interaction between the CCA treating solution and the treated wood probably involve the reduction of Cr(VI) and the concurrent oxidation of either the lignin or the hemicellulose structure. At high concentration, the dominant form of Cr(VI) is actually dichromate (i.e., already dimerized), as opposed to chromate. Any oxygen-containing functional group in the wood structure should provide a possible reaction site for the reduction of the dichromate ions. These oxidation reactions are most likely innersphere reactions, and therefore will have as their ultimate product a Cr(III) species bound to the wood structure through one or more oxygen ligands; albeit, a major shift in local coordination geometry for the Cr would occur upon reduction from the hexavalent to the trivalent state. Given that electron transfer would occur through an innersphere complex and that the resulting products have a favorable interaction, it is probable that a dimerized Cr(III) product bound to the wood tissue would result. The As(V) species would then likely attach to the Cr dimer and yield the Cr/As cluster proposed above.

Environmental Implications. The form of the Cr and As in CCA-treated material is consistent between newly manufactured and aged samples, and between treated wood and dislodgeable residue samples. In all cases, the dominant oxidation states of the two elements are As(V) and Cr(III), respectively, and the local chemical environmental of the two elements is best represented as a Cr/As cluster consisting of a Cr dimer bridged by an As(V) oxyanion. Because As(V) is the most oxidized form of As, it is unlikely that, under aerobic conditions, there would be any change in As oxidation state. Chromium(III) is thermodynamically unstable in comparison to Cr(VI) under aerobic conditions, but the presence of a large amount of organic material in the form of the wood structure and the lack of any significant Mn-oxide fraction indicate that oxidation of Cr(III) to Cr(VI) is highly unlikely.

The Cr dimer is bridged by at least one carboxyl group that serves, along with other organic ligands, to anchor the cluster to the woody structure. This implies that the two elements should be quite resistant to leaching, provided that chemical modification did not ensue and that the wood structure remains intact (i.e., degradation has yet to transpire). The long-term stability of the As/Cr cluster is further emphasized by its persistence from the new wood through the aged wood and the dislodgeable residue. Only conditions that serve to enhance either the replacement of the bridging carboxylic group with some ligand that is not an integral part of the wood structure or displacement of the As from the Cr dimer, such as the addition of acid or oxalate to the system, would be expected to enhance the release of these elements. This is consistent with recent research investigating the release of metals (arsenic, chromium, and copper) from the surface of treated wood as it weathers. A study of the concentration of metals in wipe samples that were collected over 753 days of environmental weathering reported that, for a given wood site, the fluctuation in surface concentrations of metals showed almost no change over time (*29*). These findings led to the suggestion that simple diffusion of arsenic out of the wood does not account for the constant surface concentration, and that rejuvenation of the wood surface by erosion is a primary contributor to maintaining surface arsenic concentrations (*29*). Additionally, it provides further evidence that the metals are well anchored to the wood structure and not easily mobilized under environmental conditions. Although due to the chemical similarity between Cr and Fe, and the similarity in the manor of As binding to the Cr cluster and As bound on the surface of iron oxides, it is likely that conditions previously shown to enhance As release from Fe oxides would also facilitate release of As from CCA-treated material. Because of the potential for the reduction of As(V) to As(III) under anoxic/reducing conditions, As mobility may be different under those types of conditions. Oxidative degradation of the wood structure is also likely to lead to initial mobilization of Cr and As by releasing the cluster from its attachment to the wood polymers. However, Cr would likely form either a chromium hydroxide phase, to which arsenate may bind, or adsorb on mineral surfaces (*30*, *31*). Additionally, owing to the abundance of ferric (hydr)oxides within the dislodgeable residue and most soils, coupled with the affinity of arsenic for such phases, it is anticipated that in the absence of a large fraction of mobile colloidal Fe oxides any arsenic that was released from CCA-treated wood would likely bind to stationary iron phases in the residue or soil and be rendered virtually immobile.

Acknowledgments

We thank Dr. Matthew A. Marcus of the Advanced Light Source for his invaluable assistance with the XAS-microprobe work. We also thank the American Chemistry Council for supplying the materials analyzed in this work and Georgia Pacific for providing the necessary funding. X-ray absorption spectroscopy was carried out at the Stanford Synchrotron Radiation Laboratory, a national user facility operated by Stanford University on behalf of the U.S. Department of Energy, Office of Basic Energy Sciences. The SSRL Structural Molecular Biology Program is supported by the Department of Energy, Office of Biological and Environmental Research, and by the National Institutes of Health, National Center for Research Resources, Biomedical Technology Program.

Supporting Information Available

One figure showing the correlation between Cr and As fluorescence intensity. This material is available free of charge via the Internet at http://pubs.acs.org.

Literature Cited

(1) Hingston, J. A.; Collins, C. D.; Murphy, R. J.; Lester, J. N. *Environ. Pollut.* **2001**, *111*, 53−66.
(2) Bull, D. C.; Harland, P. W.; Vallance, C.; Foran, G. J. *J. Wood Sci.* **2000**, *46*, 248−252.
(3) Bull, D. C. *Wood Sci. Technol.* **2001**, *34*, 459−466.
(4) Zagury, G. J.; Samson, R.; Deschenes, L. *J. Environ. Qual.* **2003**, *32*, 507−514.
(5) Balasoiu, C. f.; Zagury, G. J.; Deschenes, L. *Sci. Total Environ.* **2001**, *280*, 239−255.
(6) Solo-Gabrielle, H.; Townsend, T. *Generation, Use, Disposal and Management Options for CCA-treated Wood*; Florida Center for Solid and Hazardous Waste Management: 1998.
(7) Woolson, E. A.; Gjovik, L. R. The valence state of arsenic on treated wood. *Proc.—Annu. Meet. Am. Wood Preserv. Assoc.* **1981**, *77*, 15−22.
(8) Kamdem, D. P. *ESEM of CCA Type C Treated Southern Pine*; Osmose Inc.; 2001.
(9) Kamdem, D. P.; Cui, W. *X-ray Diffraction of CCA Treated Wood Surface*; Osmose Inc.; 2001.
(10) Webb, S. *SixPack*; 2002.
(11) Ressler, T. *WinXAS* v. 2.0 1997.
(12) Kelly, S. D.; Kemner, K. M.; Fryxell, G. E.; Liu, J.; Mattigod, S. V.; Ferris, K. F. *J. Phys. Chem. B* **2001**, *105*, 6337−6346.
(13) Waychunas, G. A.; Rea, B. A.; Fuller, C. C.; Davis, J. A. *Geochim. Cosmochim. Acta* **1993**, *57*, 2251−2269.

(14) Fischer, H. R.; Glerup, J.; Hodgson, D. J.; Perdersen, E. *Inorg. Chem.* **1982**, *21*, 3063−3066.
(15) Stearns, D. M.; Armstrong, W. H. *Inorg. Chem.* **1992**, *31*, 5178−5184.
(16) Nakahanada, M.; Fujihara, T.; Fuyuhiro, A.; Kaizaki, S. *Inorg. Chem.* **1992**, *31*, 1315−1316.
(17) Eshel, M.; Bino, A.; Felner, I.; Johnston, D. C.; Luban, M.; Miller, L. L. *Inorg. Chem.* **2000**, *39*, 1376.
(18) Eshel, M.; Bino, A. *Inorg. Chim. Acta* **2001**, *320*, 127−132.
(19) Eshel, M.; Bino, A. Polynuclear chromium(III) carboxylates. 3. Cyclic and cubane type hexachromium acetates. *Inorg. Chim. Acta* **2002**, *329*, 45−50.
(20) Jacquamet, L.; Sun, Y.; Hatfield, J.; Gu, W.; Cramer, S. P.; Crowder, M. W.; Lorigan, G. A.; Vincent, J. B.; Latour, J.-M. *J. Am. Chem. Soc.* **2003**, *125*, 774−780.
(21) Estes, E. D.; Scaringe, R. P.; Hatfield, W. E.; Hodgson, D. J. *Inorg. Chem.* **1976**, *15*, 1179−1182.
(22) Estes, E. D.; Scaringe, R. P.; Hatfield, W. E.; Hodgson, D. J. *Inorg. Chem.* **1977**, *16*, 1605−1610.
(23) Bino, A.; Chayat, R.; Pedersen, E.; Schneider, A. *Inorg. Chem.* **1991**, *30*, 856−858.
(24) Crimp, S. J.; Spiccia, L.; Krouse, H. R.; Swaddle, T. W. *Inorg. Chem.* **1994**, *33*, 465−470.
(25) Gardea-Torresdey, J. L.; Tiemann, K. J.; Armendariz, V.; Bess-Oberto, L.; Chiamelli, R. R.; Rios, J.; Parsons, J. G.; Gamez, G. *J. Hazard. Mater. B* **2000**, *80*, 175−188.
(26) Parsons, J. G.; Hejazi, M.; Tiemann, K. J.; Henning, J.; Gardea-Torresdey, J. L. *Microchem. J.* **2002**, *71*, 211−219.
(27) Yun, Y.-S.; Park, D.; Park, J. M.; Volesky, B. *Environ. Sci. Technol.* **2001**, *35*, 4353−4358.
(28) Flogeac, K.; Guillon, E.; Marceau, E.; Aplinecourt, M. *New J. Chem.* **2003**, *27*, 714−720.
(29) Stilwell, D.; Toner, M.; Sawhney, B. *Sci. Total Environ.* **2003**, *312*, 123−133.
(30) Hansel, C. M.; Fendorf, S. E.; LaForce, M. J.; Sutton, S. *Environ. Sci. Technol.* **2002**, *36*, 1988−1994.
(31) LaForce, M. J.; Hansel, C. M.; Fendorf, S. e. *Environ. Sci. Technol.* **2000**, *34*, 3937−3934.
(32) Zabinsky, S. I.; Rehr, J. J.; Ankudinov, A.; Albers, R. C.; Eller, M. J. Multiple scattering calculations of X-ray absorption spectra. *Phys. Rev. B* **1995**, *52*, 2995.

Received for review October 10, 2003. Revised manuscript received June 8, 2004. Accepted July 7, 2004.

ES0351342